Electrical Engineering in Japan, Vol. 138, No. 3, 2002
Translated from Denki Gakkai Ronbunshi, Vol. 121-B, No. 1, January 2001, pp. 8–14

Quantitative Evaluation of Generator Power Control Effect of FACTS Controllers for Power System Stabilization

MASAHIDE HOJO,[1] YASUNORI MITANI,[2] TOSHIFUMI ISE,[2] and KIICHIRO TSUJI[2]
[1]Department of Electrical and Electronic Engineering, The University of Tokushima, Japan
[2]Department of Electrical Engineering, Osaka University, Japan

SUMMARY

The advancement of power electronics technologies has significantly developed the power system stabilizing controllers. Quantitative as well as qualitative evaluation of their effectiveness in power systems is a matter of great importance for the feasibility investigation of these apparatus. In this paper, the possible control region of FACTS controllers with series and/or shunt configuration in a single machine to infinite bus system is formulated in the power-angle curve with a set of algebraic equations. The effectiveness of TCPST (Thyristor-Controlled Phase Shifting Transformer), SSSC (Static Synchronous Series Compensator), and TCSC (Thyristor-Controlled Series Compensator) for the improvement of the transient stability is evaluated quantitatively as a numerical example. The correctness of the proposed method has been confirmed by analysis based on the electromagnetic transients simulation with a detailed system model. © 2001 Scripta Technica, Electr Eng Jpn, 138(3): 43–51, 2002

Key words: FACTS; generator power control; power-angle curve; power system stabilizing control.

1. Introduction

With rapid development of power electronics technologies, power system controllers have become more and more intelligent, with the support of a great deal of impressive research. The new concepts associated with the Flexible AC Transmission System (FACTS) [1] have provided a strong forward impetus in this field. The new power system controller, which is defined as the FACTS controller [2], can control some system variables such as power flow or line impedance quickly and smoothly, so it is expected to solve problems of today's power systems [3].

FACTS controllers can be classified into three categories: series-connected controllers, shunt-connected controllers, and combined shunt-and-series-connected controllers. The Static Synchronous Series Compensator (SSSC) [4] and Thyristor-Controlled Series Compensator (TCSC) [5] are classified as series-connected-controllers. The SSSC can insert voltage in series with a transmission line by a voltage-source inverter, and the TCSC can compensate a line impedance by series capacitor and thyristor switched parallel reactor. These controllers are expected to realize some advanced power system control strategies because the controllers can regulate power flow directly and quickly. On the other hand, SVC and SMES are classified as shunt-connected controllers. The SVC has been installed on a power system through some field tests. Moreover, some controllers combined with these shunt and series connected controllers have also been proposed, for example, the Thyristor-Controlled Phase Shifting Transformer (TCPST) [6] which has a phase shifting transformer whose voltage is provided by line voltage through a line-commutated shunt inverter, Unified Power Flow Controller (UPFC) [7] which is configured series and shunt inverter sharing their DC capacitor, and SuperSMES [8] which is UPFC with SMES.

In this paper, it is assumed that the FACTS controller is used as a power flow controller for power system stabilizing control. Kato and colleagues [9] evaluated qualitatively the UPFC's capability of power flow control corresponding to its control modes by power-angle curves. However, in general, the control capabilities of FACTS controllers have been evaluated individually, so we have no universal method of evaluating the capabilities in order to make a proper comparison among the FACTS controllers without accounting for their configurations or types of connection to the power system.

Assuming that power flow control by the FACTS controller is applied to the power system stabilizing control at a long-distance power transmitting part of the system,

DOI 10.1002/eej.1127

this paper proposes a control region of FACTS controller which is useful for evaluation of its power flow control capability. The control regions can be determined for various FACTS controllers by means of representing relations between the generator output power and operating variables of the FACTS controller in power-angle plane. They express clearly the generator power variation caused by operated quantity of the operating variables of the FACTS controllers at any rotor angle and are also available in transient state analysis assuming that the control response of the FACTS controller is sufficiently quick in comparison to the dynamics of the rotor. They can be easily determined by solving a set of algebraic equations numerically, which is derived with a power system model represented by rms values including the voltage and current source representing the FACTS controller. They allow us to evaluate the control capabilities of various FACTS controllers and make comparisons among them, and, moreover, they are useful as indices when we choose a FACTS controller suitable for required control effect. The control region is also confirmed by electromagnetic transients simulation with a detail power system model.

2. Calculation of Control Region by FACTS Controller

2.1 Control effect by generator power control

A power-angle locus stabilized by generator power control is depicted on a power-angle plane. The power system model consists of a one-machine infinite-bus system and Park's generator model, taking account of field winding effects. The power swing equations can be represented as follows:

$$\frac{d\delta}{dt} = \Delta\omega \tag{1}$$

$$\frac{M}{\omega_r}\frac{d\omega}{dt} + \frac{D}{\omega_r}\Delta\omega = P_m - (P_{e0} + P_e') \tag{2}$$

$$P_{e0} = \frac{e_q' V_\infty}{x + x_d'}\sin\delta \tag{3}$$

$$-\frac{(x_q - x_d')V_\infty^2}{(x + x_d')(x + x_q)}\sin\delta\cos\delta \tag{4}$$

$$x = x_t + x_L \tag{5}$$

where δ is the rotor angle and Δω is the deviation of the rotor angle speed from zero. P_e' is the deviation of the generator power, which represents the control effect produced by some generator power controller. V_∞ and x_L denote the voltage of the infinite bus and the total amount of the line reactance, respectively, and the other constants are summarized in Table 2 (see Section 3).

Assuming that a power system stabilizing control is applied, there is an increase of the damping coefficient of the generator with regulation of the generator power by P_e'. This control strategy is termed a damping control in the following discussion. Control dynamics of the generator power controller is assumed as follows:

$$T_c\frac{dP_e'}{dt} = D'\Delta\omega - P_e' \tag{6}$$

where T_c is the time constant of the controller.

Figure 1 shows a transient response of the power system in the power-angle plane, where system constants described in Table 2 are used and a disturbance is assumed whereby a three-phase short circuit is continued in three cycles. From Fig. 1, it can be seen that the locus becomes a clockwise spiral around the equilibrium point by P_e' and finally converges into it, resulting in stabilization of the power system. The results mean that one can see clearly the stabilizing process of the power system by the damping control with the generator power increased and decreased across the power-angle curve.

2.2 Formulation of generator power control effect by FACTS controller

The FACTS controller is suitable for realizing the generator power control P_e' discussed in the previous section, because it can control the power flow on the transmission line quickly and smoothly. The purpose of this subsection is to discuss a method of formulating the relations between operating variables of various FACTS controllers and the regulated generator output power in the power-angle plane.

The control effects of the FACTS controller can be represented by a combination of variable voltage $\dot{V}_s$ inserted in series with the transmission line, which represents the control effect of the series converter, and variable current $\dot{I}_p$ supplied to the power system, which represents the con-

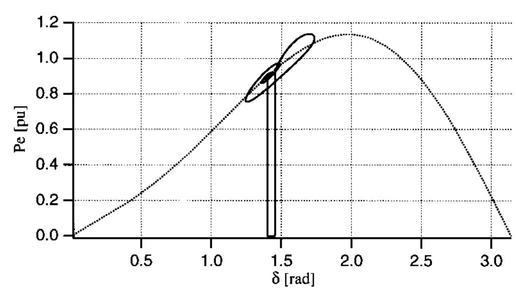

Fig. 1. Power-angle locus with the power-angle curve.

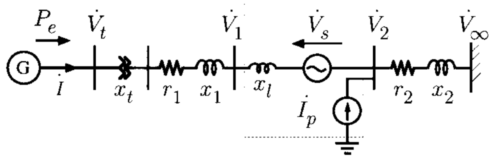

Fig. 2. Power system model with a FACTS controller.

trol effect of the shunt converter. First, generator power control effect of the FACTS controller is formulated for a single-machine–infinite-bus system which has a FACTS controller on its transmission line shown in Fig. 2.

The FACTS controller is modeled by a series voltage source V_s, shunt current source I_p, and a leakage reactance of the series transformer x_l, and any losses in the FACTS controller are neglected. When Park's model including a field winding is used to describe the dynamics of the generator, the relations between the voltage and current in the power system are represented by

$$v_d = -r_a i_d + x_q i_q \quad (7)$$

$$v_q = -r_a i_q - x'_d i_d + e'_q \quad (8)$$

$$v_d = r_1 i_d - (x_t + x_1 + x_l) i_q + v_{sd} + v_{2d} \quad (9)$$

$$v_q = (x_t + x_1 + x_l) i_d + r_1 i_q + v_{sq} + v_{2q} \quad (10)$$

$$v_{2d} = r_2(i_d + i_{pd}) - x_2(i_q + i_{pq}) + V_\infty \sin\delta \quad (11)$$

$$v_{2q} = x_2(i_d + i_{pd}) + r_2(i_q + i_{pq}) + V_\infty \cos\delta \quad (12)$$

where $\dot{V}_t$, $\dot{V}_\infty$, r_m, and $x_m (m = 1, 2)$ represent the generator terminal voltage, infinite-bus voltage, resistance and reactance of the transmission line, respectively, and other constants used in the above equations are defined as shown in Table 2. Subscript d and q refer to each component of the corresponding axis, respectively.

Assuming that power flow control by the FACTS controller is sufficiently quick in comparison to the dynamics of the rotor which depends on the inertia of the generator, the rotor angle δ is considered to be constant during the operation of the FACTS controller. In addition, dynamic response of e'_q depends on the time constant T'_{do} and is usually large between 5 and 10 seconds, so e'_q is also dealt with as constant during operation of the FACTS controller. Under these consumptions, Eqs. (7) to (12) include 10 unknown variables as follows:

$$\boldsymbol{\xi} = [v_d, v_q, i_d, i_q, v_{2d}, v_{2q}, v_{sd}, v_{sq}, i_{pd}, i_{pq}]^T \quad (13)$$

Of these variables, four v_{sd}, v_{sq}, i_{pd}, and i_{pq}—represent output of the FACTS controller, so the variables are used as operating variables or determined by some additional constraints due to the configuration and the control system of the FACTS controller. With these considerations about FACTS controller, four equations are added to the above six equations.

For example, SuperSMES [8] can control the four operating variables separately. On the other hand, UPFC does not have a large energy storage sufficient to trade active power between the utility and the controller, so we can design a control system using three variables independent of each other and the following constraint should be added:

$$v_{sd} i_d + v_{sq} i_q = v_{2d} i_{pd} + v_{2q} i_{pq} \quad (14)$$

Next, the control region of FACTS controller is determined by the procedure discussed above. In this paper, three FACTS controllers—TCPST, SSSC, and TCSC—are used as examples. Operating variables and constraints about each FACTS controller are considered as follows.

Regarding the TCPST, the voltage conversion ratio n (n is assumed to be a real number) is an operating variable, which is defined as the ratio of the variable voltage $\dot{V}_s$ inserted in series with the transmission line to the voltage $\dot{V}_2$ at the bus to which the TCPST is connected. $\dot{V}_s \perp \dot{V}_2, \dot{I}_p \perp \dot{I}$, and Eq. (14) are introduced as additional constraints because the TCPST, like the UPFC, does not have a sufficient energy storage.

The SSSC inserts its output voltage $\dot{V}_s$ in series with the transmission line, whose magnitude V_s is an operating variable, and whose phase is kept quadrature with the line current. As the SSSC trades no active power with the power system, it can be modeled as a series voltage source only. Thus, the constraints can be represented as $\dot{V}_s \perp \dot{I}$ and $\dot{I}_p = 0$. It is noted that the two equations always satisfy Eq. (14).

For the TCSC, although the equivalent reactance X_c should be an operating variable, the TCSC can be modeled as a series voltage source whose output voltage is the same as a voltage drop across the TCSC caused by its operation. As a result, $\dot{V}_s = jX_c\dot{I}$ and $\dot{I}_p = 0$ are added to the constraints. In this case, Eq. (14) is also satisfied.

These results are summarized in Table 1. The power system model shown in Fig. 2 can be precisely formulated by 10 equations, which consist of Eqs. (7) to (12) and 4 equations shown in Table 1 depending on the FACTS controller. By solving these 10 equations numerically, unknown variables ξ can be determined corresponding to the given values of δ, e'_q, and the operating variable n (or V_s, X_c). The generator power P_e can also be determined by substituting i_d, i_q of ξ for

$$P_e = \{(x_q - x'_d) i_d + e'_q\} i_q \quad (15)$$

Table 1. Constraints by FACTS controllers

FACTS controller	TCPST	SSSC	TCSC
Operating Variable	voltage conversion ratio n	magnitude of series voltage V_s	equivalent reactance X_c
constraints	$v_{sd} + nv_{2q} = 0$	$i_{pd} = 0$	$i_{pd} = 0$
	$v_{sq} - nv_{2d} = 0$	$i_{pq} = 0$	$i_{pq} = 0$
	$i_{pd} - ni_q = 0$	$0 = v_{sd}i_d + v_{sq}i_q$	$v_{sd} = -X_c i_q$
	$i_{pq} + ni_d = 0$	$V_s = \sqrt{v_{sd}^2 + v_{sq}^2}$	$v_{sq} = X_c i_d$

Where the SSSC is used, it is noted that P_e can be determined as only one value when $V_s = 0$ but $V_s > 0$ should lead to two values of P_e, one of them larger than the value when we solved with $V_s = 0$ and the other smaller than the value. These two values of P_e depend on the relation of phase between the output voltage $\dot{V}_s$ and the line current $\dot{I}$, that is, the former corresponds to the case of $\dot{V}_s$ lagging $\dot{I}$ by 90° and the latter corresponding to the case of $\dot{V}_s$ leading $\dot{I}$ by 90°.

Usually the FACTS controller is operated within the limits of the operating variable which depends on its capacity. For each of the FACTS controllers considered above, the limits of the operating variable can be represented by the maximum allowable value of the operating variable U ($U > 0$) as follows:

$$-U \le n \le U \quad \text{(in the case of TCPST)} \tag{16}$$

$$0 \le V_s \le U \quad \text{(in the case of SSSC)} \tag{17}$$

$$-U \le X_c \le U \quad \text{(in the case of TCSC)} \tag{18}$$

On the other hand, the rotor angle δ is commonly considered with $0 \le \delta \le \pi$.

By the two parameters—the rotor angle δ and the operating variable of the FACTS controller limited within each limit—a set of P_e can be determined as a region in the power-angle plane. The region is defined as a control region by the FACTS controller.

3. Evaluation of Control Effect of FACTS Controllers by Control Region

With the power system model shown in Fig. 2 and constants shown in Table 2, control regions of some FACTS controllers are investigated by the method of the previous section.

The resistance of the transmission line is assumed to be $r_a = r_1 = r_2 = 0$ for simplicity, and e_q' is defined as a constant value which is derived by power flow calculations with $P_e = 0.9$ pu, $V_t = 1.0$ pu, and $v_\infty = 1.0$ pu. $x_l = 0$ is used for the TCSC because it does not have a series transformer. Figures 3 to 5 show the results. In each figure, the hatched area is the control region derived by solving the set of Eqs. (16) to (18) with U = 0.2 pu, and the power-angle locus obtained in the previous section is also depicted.

Assuming that the control response of the FACTS controller is quick in contrast to the dynamics of the rotor, these control regions show the values of P_e which can be

Table 2. System constants

Generator (4000-MVA base, model with e_q' constant)	
inertia constant M [s]	7.527
damping coefficient D [pu]	0.0
added damping coefficient by the damping control D' [pu]	0.05
d-axis reactance x_d [pu]	1.79
d-axis transient reactance x_d' [pu]	0.355
q-axis reactance x_q [pu]	1.66
Transmission line and FACTS controller (4000-MVA, 500-kV base)	
reactance of transformer in the power station x_t [pu]	0.15
line reactance x_1 [pu]	0.0
line reactance x_2 [pu]	0.3852
leakage reactance of series transformer x_l [pu]	0.100
time constant of power flow controller T_c [s]	0.05

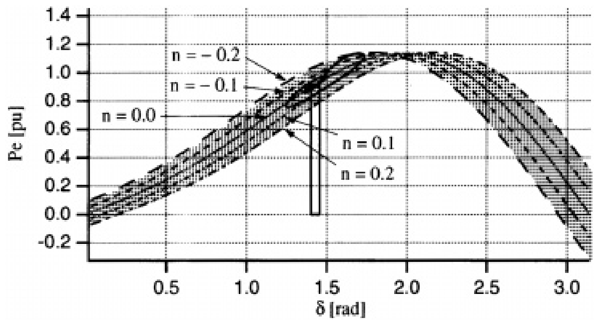

Fig. 3. Relations between power-angle curve and output voltage of TCPST.

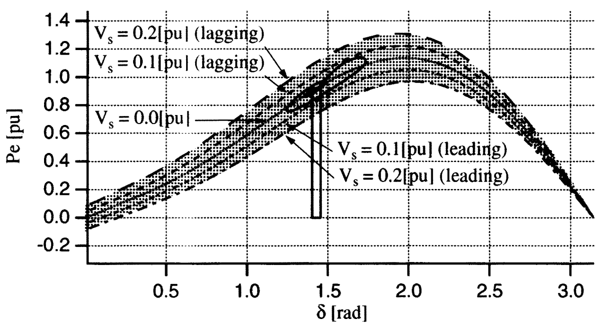

Fig. 4. Relations between power-angle curve and output voltage of SSSC.

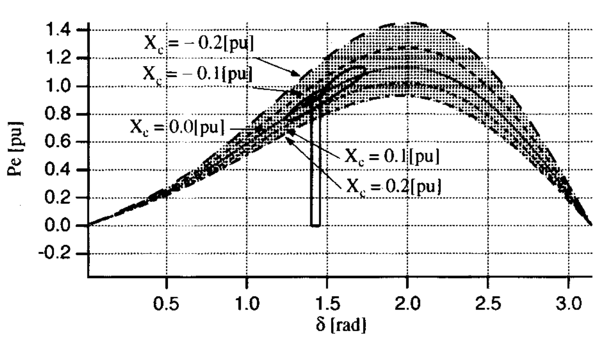

Fig. 5. Relations between power-angle curve and control output of TCSC.

settled by the operation of the FACTS controller corresponding to rotor angle δ whether the generator is in steady or transient state. As a result, the following consideration is available using these control regions.

First, we can easily estimate the minimum operating capability of the FACTS controller required for the purpose of realizing desired power system stabilizing control, and, moreover, make a comparison between various FACTS controllers. In order to realize the damping control discussed in the previous section, for example, the FACTS controller with a control region which can include the power-angle locus should be used. From Figs. 3 to 5, we can easily determine the FACTS controller and required operating limits, that is, TCPST with $U = 0.2$ pu, SSSC with $U = 0.1$ pu, or TCSC with $U = 0.1$ pu can be applied to the power system for realizing damping control. This method can also be applied to other control strategies using the generator power control.

Next, the control region allows a comparison between FACTS controllers based an quantitative evaluation of its control effect at each operating point of the power system. The control effect of the TCSC, for example, is decreased when the generator outputs small power as shown in Fig. 5, but when the generator outputs large power, the control effect of the TCPST is decreased. On the other hand, the control effect of the SSSC is not affected by the generator output power with its control region large, and therefore can realize some effective controls. The control region can be a useful index for selection of FACTS controller which is suitable around its operating point.

In the above examples, FACTS controllers are evaluated based on the power-angle locus, but the locus was obtained by some generator power control (6). Actually, if one of the FACTS controllers has already been considered for use and its capacity decided, it is possible that someone may wish to investigate usage of other FACTS controllers. In such cases, starting with taking into account a concrete FACTS controller and its behavior when the power-angle locus is determined as shown in Fig. 1, one can process the investigation by a method as follows.

We now assume that one has the results obtained by the control of the TCSC where the operating limit is also considered, based on detailed and practical investigation. When the results are plotted in the power-angle plane, the locus ought to be limited within the control region of the TCSC. The limitations of the locus reflect the operating limit of the TCSC. Consequently, one can evaluate control effects by other FACTS controllers based on their control regions with the limited locus, and, as a result, make a comparison between the FACTS controllers including their operating limits. It is noted that the influences of the operating limit on the shape of the control region differ according to the FACTS controller, and therefore the evaluation results include errors caused by it.

It can be regarded that evaluations based on the control region are corrupted by considering the AVR dynamics and using a detailed generator model because the control region is derived with e_q' constant. However, the maximum value of generator power deviation produced by the FACTS controller, which is used for calculation of the operated quantity by it, usually appears as soon as fault clearance occurs. Therefore, variation of e_q' hardly influences the evaluation results based on the control region.

As shown here, the proposed control region can be a useful method of investigating required operating quantity and making a comparison between FACTS controllers based on the same standard. Adding analysis by transient simulations to the evaluation results, we can improve the precision.

4. Experimental Confirmation of Control Region by Electromagnetic Transients Simulation

In previous sections, dynamic response of rotor angle δ and e_q' is assumed to be constant because those values are sufficiently slower than the control response by the FACTS controller. In this section, in order to confirm a control region derived numerically by the process discussed in Section 2, it is compared with experimental results obtained by repetition of electromagnetic transients simulation using a detailed power system model with AVR and governor shown in Fig. 6.

Figure 6 shows the system model used by the electromagnetic transients simulation program (PSCAD/EMTDC [10]), which presents exactly the same behavior as an experimental power system model [11]. The model simulates a transmission line whose line-to-line voltage rating is 500 kV and which is sending power to a large-scale interconnected power system which is 240 km from the power plant. The power plant which has two 1000-MVA-class generators is modeled as a single generator with AVR and speed governor. Assuming that the SSSC causes no loss in its circuit and its DC voltage is kept constant by some control, it is simulated as three single-phase PWM inverters inserted in series with each phase of the transmission line, whose DC side is connected to the same constant DC voltage source. Constants of the power system are shown in Table 3.

First, a transient response of the generator power is observed, caused by a system disturbance whereby a three-phase short circuit fault at point F occurred at t = 2.0 s, continued in t_f [s], and finally diminished resulting in the initial state of the system.

By repeated simulation varying t_f, the critical clearing time without the SSSC control was calculated as 0.19 s. That is, when t_f = 0.19, the rotor of the generator presented the biggest swing around the equiribrium point without becoming unstable, and transient responses of generator power P_e and rotor angle δ are shown by the dashed line in Fig. 7(a).

Next, the response of generator power P_e controlled by the SSSC was investigated, where the output voltage of the SSSC changed so as to step up from zero to its maximum value at some time ($t = t_a$ s, $2.19 < t_a < 3.5$) in the transient state. Figure 7(a) shows, for example, a set of simulated results by the solid line obtained when the output voltage of the SSSC was changed from zero to 0.6 pu lagging the line current by 90° at t_a = 3.0 s. The generator power P_e settled onto the dot-dash line in about 50 ms with overshoot as shown in Fig. 7(b). However, the rotor angle δ changed very little by the control of the SSSC from the value δ = 2.46 rad at t = 3.0 s. From these results, the control effect of the generator power by the SSSC can be determined as an amount of generator power changed by the SSSC, ΔP_e = 0.25 pu, as shown in Fig. 7(b). Figure 7(b) also shows that v_{sU} lagged i_U by 90°, where the subscript U means the variable is of phase U. As a result, we can plot a point (δ, P_e) = (2.46, 1.18) in the power-angle plane as the control effect by the SSSC at δ =

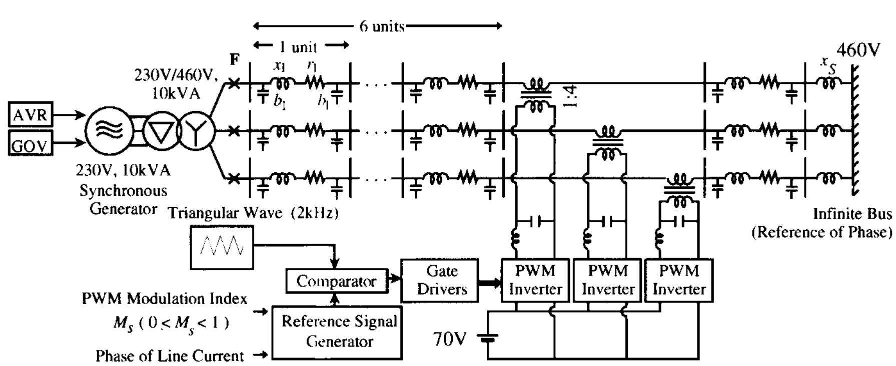

Fig. 6. Detailed power system model with SSSC.

Table 3. System constants

Generator parameters (10-kVA generator capacity base)	
armature resistance r_a [pu]	0.046
portier reactance x_p [pu]	0.26
d-axis reactance x_d [pu]	1.35
d-axis transient reactance x'_d [pu]	0.48
d-axis sub-transient reactance x''_d [pu]	0.27
damper-field mutual reactance x_{kf} [pu]	0.05
q-axis reactance x_q [pu]	1.31
q-axis transient reactance x'_q [pu]	0.27
armature time constant T_a [s]	0.020
d-axis transient time constant T'_{do} [s]	0.21
d-axis sub-transient time constant T''_{do} [s]	0.020
q-axis transient time constant T''_{qo} [s]	0.020
inertia constant M [s]	7.75
Power system parameters (10-kVA, 460-V base)	
line reactance (per 1 unit) x_1 [pu]	0.046
line resistance (per 1 unit) r_1 [pu]	0.005
line capacitance (per 1 unit) b_1 [pu]	0.027 × 2
reactance of transformer x_t [pu]	0.15
leakage reactance of series transformer x_l [pu]	0.10
reactance modified the interconnected power system x_s [pu]	0.092

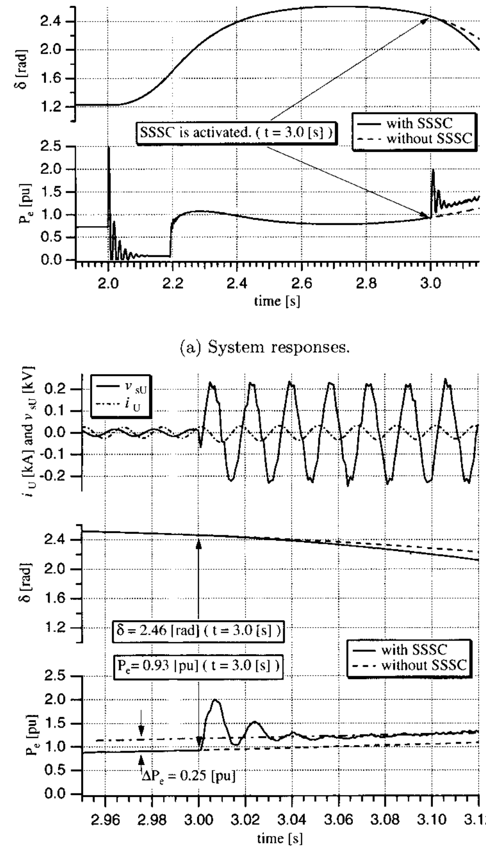

(a) System responses.

(b) System responses (magnified).

Fig. 7. Power flow control by SSSC simulated with PSCAD/EMTDC program.

2.46 confirmed by the electromagnetic transients simulation, as shown in Fig. 4.

The simulation discussed above was repeated varying t_a, the time changing the output voltage of the SSSC, so that Fig. 4 summarizes the results. A part of the power-angle curve corresponding to $\delta > 2.6$ rad could not be obtained by the electromagnetic transients simulation because the generator power response could not be settled until the system lost synchronism in contrast to the results shown in Fig. 7(b).

Figure 4 also shows the results derived by the numerical method proposed in Section 2. The detailed power system model is simplified as shown in Fig. 2 and the system constants summarized in Table 3 are used for solving Eqs. (7) to (12), where the resistances included in the system are neglected for simplicity. The constant value of e'_q is obtained by the power flow calculation with $V_s = 0$ pu, $P_e = 0.7$ pu, and $V_t = 1.0$ pu.

Although it can be seen that the difference between two results is due to control by the AVR and governor, Fig. 4 shows that the two results almost agree with each other. Therefore, the control region is confirmed by the electromagnetic transients simulation with detailed power system model.

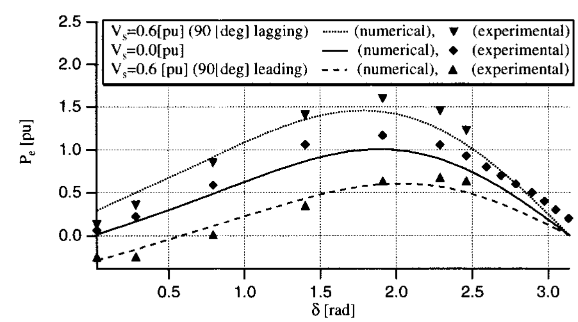

Fig. 8. Power-angle curve (simulated with PSCAD/EMTDC program).

5. Conclusions

This paper has proposed the control region in the power-angle plane as a universal index for evaluating the generator power control capability of FACTS controllers for power system stabilization. The obtained results are summarized below.

1. Starting with modeling the FACTS controller as a series voltage source and shunt current source, relations between controlled generator output power and operated quantity of the FACTS controller are determined as a control region in the power-angle plane for power system stabilizing control based on generator power control.

2. By the proposed control region, control ability of the FACTS controller with respect to the operating point of the system can be made clear and evaluated quantitively; therefore, we can determine the FACTS controller suitable for the operating point of the system, and see the capacity of the FACTS controller required to realize desired control easily.

3. By the electromagnetic transients simulation with detail power system model including the generator control system, the proposed control region is available in both steady and transient state. From these results, the proposed control region provides a useful method of evaluating the effectiveness of the FACTS controller quantitatively for generator power control.

Acknowledgment

I thank Junnichi Ishii, who now works for Fuji Electric Co., for giving me helpful suggestions while he was with the Department of Electrical Engineering, Graduate School of Engineering, Osaka University.

REFERENCES

1. Hingorani NG. High power electronics and flexible AC transmission system. IEEE Power Eng Rev, p 3–4, July 1988.
2. Edris AA, et al. Proposed terms and definitions for flexible AC transmission system (FACTS). IEEE Trans Power Delivery 1997;12:1848–1853.
3. IEEE Power Engineering Society. FACTS applications. IEEE 96 TP 116-0, 1996.
4. Sen KK. SSSC—Static synchronous series compensator: Theory, modeling, and applications. IEEE Trans Power Delivery 1998;13:241–246.
5. Kato K, Morioka Y, Mishima Y, Nakachi Y, Asada M, Watanabe M, Konishi H. Development of a thyristor-controlled series compensator for a simulator. Trans IEE Japan 1997;117-B:1016–1023. (in Japanese)
6. Iravani MR, Dandeno PL, Nguyen KH, Zhu D, Maratukulam D. Applications of static phase shifters in power systems. IEEE Trans Power Delivery 1994;9:1600–1607.
7. Gyugi L, Schauder CD, Williams SL, Rietman TR, Torgerson DR, Edris A. The unified power flow controller: A new approach to power transmission control. IEEE Trans Power Delivery 1995;10: 1085–1097.
8. Kamolyabutra D, Hojo M, Mitani Y, Ise T, Tsuji K. Experimental study on power system stabilizing control scheme for the SMES with solid-state phase shifter (Super SMES) using local signals. Trans IEE Japan 1999;119-B:581–588. (in Japanese)
9. Kato M, Morioka Y, Nakahigashi Y, Mishima Y, Nakachi Y, Asada M, Tokuhara K, Akamatsu M, Furuta M. Implementation of unified power flow controller and verification for transmission capability improvement. Trans IEE Japan 1998;118-B:1194–1200. (in Japanese)
10. Nayak O, Irwin G, Neufeld A. GUI enhances electromagnetic transients simulation tools. IEEE Comput Appl Power 1995;8:17–22.
11. Ise T, Hayashi T, Ishii J, Kumagai S. Power system stabilizing control using high speed phase shifter (HSPS). Proc PCC-Nagaoka '97, p 735–740.

AUTHORS (from left to right)




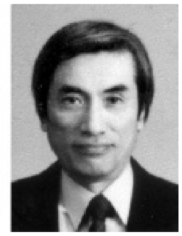

Masahide Hojo (member) received his B.S. and M.S. degrees in electrical engineering from Kobe University in 1994 and 1996, and D.Eng. degree in electrical engineering from Osaka University in 1999. He joined the Department of Electrical and Electronic Engineering of the University of Tokushima and is currently an assistant there. He is a member of the Institute of Systems, Control and Information Engineers and IEEE.

Yasunori Mitani (member) received his B.S., M.S., and D.Eng. degrees in electrical engineering from Osaka University in 1981, 1983, and 1986. He joined the Low Temperature Center, Osaka University, and the Department of Electrical Engineering, Osaka University, in 1988 and 1990. He is currently an associate professor there. His research interests are in the areas of analysis and control of power systems. He is a member of the Institute of Systems, Control and Information Engineers and IEEE.

Toshifumi Ise (member) received his B.S., M.S., and D.Eng. degrees in electrical engineering from Osaka University in 1980, 1982, and 1986. He joined Nara National College of Technology and the Department of Electrical Engineering, Osaka University, in 1986 and 1990. He is currently an associate professor there. His research interests include power converter for superconducting magnetic energy storage (SMES), power quality control by using SMES, new power distribution system (FRIENDS), and unbundled power quality service. He is a member of the Institute of Systems, Control and Information Engineers, the Japan Society for Power Electronics, and IEEE.

Kiichiro Tsuji (member) received his B.S. and M.S. degrees in electrical engineering from Osaka University in 1966 and 1968, and his Ph.D. degree in systems engineering from Case Western Reserve University in 1973. He then joined the Department of Electrical Engineering, Osaka University, and is currently a professor there. His research interests are in the areas of analysis, planning, and evaluation of energy systems including electrical power systems. He is a member of the Japan Society of Energy and Resources, the Society of Instrument and Control Engineers, the Institute of Systems, Control and Information Engineers, and IEEE.